The Abdus Salam
International Centre for Theoretical Physics

United Nations
Educational, Scientific
and Cultural Organization

International Atomic
Energy Agency

H4.SMR/1775-29

"8th Workshop on Three-Dimensional Modelling of
Seismic Waves Generation, Propagation and their Inversion"

25 September - 7 October 2006

# Subcratonic low-velocity layer and flood basalts

*Lev Vinnik*

Institute of Physics of the Earth
Moscow, Russia

GEOPHYSICAL RESEARCH LETTERS, VOL. 29, NO. 4, 10.1029/2001GL014064, 2002

# Subcratonic low-velocity layer and flood basalts

Lev Vinnik[1]
Institute of Physics of the Earth, Moscow, Russia

Veronique Farra
Institut de Physique du Globe de Paris, Paris, France

Received 11 September 2001; revised 22 November 2001; accepted 25 January 2002; published 28 February 2002.

[1] Teleseismic recordings of several seismograph stations are processed with the aid of the S receiver function technique [*Farra and Vinnik*, 2000]. The data provide evidence of a strong reduction of S velocity at a depth around 360 km (station BOSA) and 280–300 km (station LBTB) in the East of southern Africa. A similar feature is found in the Tunguska basin of the Siberian platform from the recordings of station NRIL. In both regions large volumes of flood basalts have been erupted 190–180 Ma and 250 Ma ago, respectively. The coincidence suggests a causal relation between the two phenomena. This relation implies that the low-velocity anomalies migrate with the plates. *INDEX TERMS:* 7218 Seismology: Lithosphere and upper mantle; 8121 Tectonophysics: Dynamics, convection currents and mantle plumes; 8124 Tectonophysics: Earth's interior—composition and state; 8147 Tectonophysics: Planetary interiors (5430, 5724)

## 1. Introduction

[2] The Kaapvaal and Zimbabwe cratons in southern Africa, like the other Precambrian platforms, are underlain by a high-velocity mantle root that may extend to a depth of 250–300 km [*James et al.*, 2001]. No low-velocity layer is found between the Moho and 410-km depth [*Freibourger et al.*, 2001]. However, a low S velocity layer with the top at a depth around 360 km has been detected in the same region with the aid of the P-to-S converted phases (Ps) [*Vinnik et al.*, 1996]. This feature, if real, may have important implications for processes in the upper mantle. Now we investigate deep structure of southern Africa (Figure 1) with the aid of the S-to-P converted phases (Sp), that are detected with the S receiver function technique [*Farra and Vinnik*, 2000]. The Ps converted phases from deep discontinuities can be distorted by multiple reflections and scattering from shallow discontinuities, but the Sp phases arrive earlier than the multiples.

## 2. S Receiver Function Technique

[3] The idea is to standardize the S waveforms of many seismic events and to detect the Sp phases by stacking of many recordings with moveout time corrections in a broad epicentral distance interval. The recorded seismograms are decomposed into the P, M and O components. The P axis which is optimal for observing Sp phases is perpendicular to the principal particle motion direction of the S wave in the vertical plane containing the source and the receiver. Axis M corresponds to the principal motion direction of the S wave in the horizontal plane, and axis O is perpendicular to M in the horizontal plane. The P components are deconvolved by the M components.

[4] For the group of N recordings at the same seismograph station we can define the misfit function $E$ to be minimized:

$$E(t) = \Sigma_{i=1}^{N} w_1^2 [P_i(t) - P_c(t)\cos\Delta\theta_i - P_s(t)\sin\Delta\theta_i]^2,$$

[5] .Where $t$ is time, $P_c(t)$ and $P_s(t)$ are unknowns to be determined, $P_i(t)$ is the $P$ component of event (i) deconvolved by the M component of the S wave, $\Delta\theta_i = \phi_i + \pi - \theta_i$, $\phi_i$ is back azimuth of the i-th event, $\theta_i$ is azimuth of the axis M, $w_i^2 = 1/\sigma_i^2$, and $\sigma_i^2$ is the variance of noise in the i-th record. $P_c(t)$ is the P component (observed at the free surface) corresponding to the incident $SV$ and deconvolved by the $SV$ observed at the free surface. Meaning of $P_s(t)$ is more complicated, and it will not be considered here. The solution for $P_c(t)$ is equivalent to stacking of $P_i(t)$ with weights depending on $w_i$ and $\Delta\theta_i$.

## 3. Data and Results

[6] The most important observation has been made at station BOSA (Figure 1), and these data will be presented in further detail. The results of stacking of $P_i(t)$ are shown in Figure 2. Time shifts for stacking are obtained as a product of differential slowness (the difference between the assumed slowness and the slowness of S) and differential distance (the difference between the epicentral distance of the event and the reference distance). To suppress noise the raw records were low-pass filtered with a corner at around 8 s.

[7] In the back azimuth sector of 30°–60° we have processed the records of 31 events, almost all of them in the epicentral distance range of 70°–90°. For the list of representative events see Table 1. The other back azimuth sector with a sufficient amount of suitable recordings (54) is between 230° and 260°. Epicentral distances are from 75° to 104°. The stack for the first azimuth demonstrates two clear phases: one at a time around −5 s with a differential slowness of 0.0 s/deg, and the other, at a time of −45.0 s and a slowness of 0.6 s/deg. Polarities of the two phases are opposite, and the amplitudes (amplitude ratios between the signal and the SV component of S) are 0.17 and 0.045, much larger than the standard error (0.009) of the estimate of $P_c$. The error is evaluated for a time interval a few tens of seconds long where the phases of interest are expected to arrive. The former signal is the Sp phase from the Moho. Inverse polarity of the second phase indicates that it is converted from the S velocity decreasing with depth. In the stack for the second azimuth there are two clear Sp phases: from the Moho and from '410 km' discontinuity (at −50 s). The phase with the inverse polarity and the related low-velocity layer are absent.

[8] To invert the signal that arrives at −45.0 s for the related mantle structure, we synthesized theoretical seismograms for the same distances, back azimuths, depths and focal plane solutions, as

[1]Also at GeoForschungsZentrum Potsdam, Potsdam, Germany.


0094-8276/02/2001GL014064$05.00

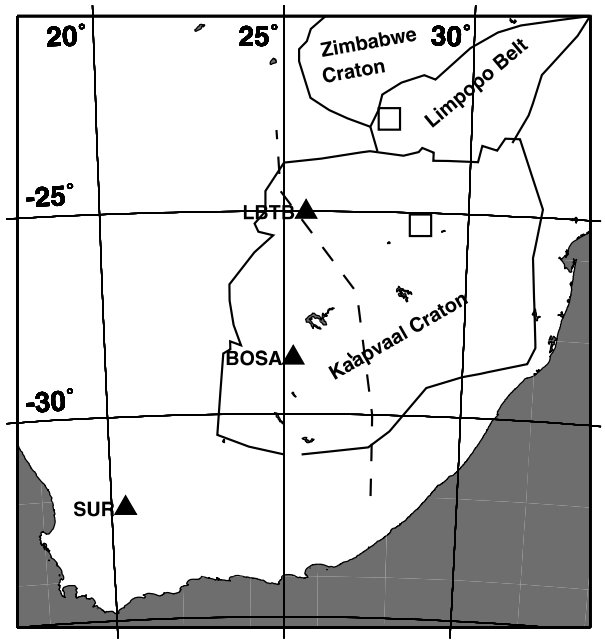


**Figure 1.** Map of the region. Squares indicate approximate positions of the centers of the regions, where low S velocity was inferred from the data of stations BOSA and LBTB. Outcrops of Karoo basalts are known only to the East of the dash line.

in the actual data, and processed them, like the actual recordings. The synthetics were calculated with reflectivity technique [*Fuchs and Mueller*, 1971]. The stacked synthetics and the related S velocity models are shown in Figure 3 and Figure 4, respectively. For the standard model IASP91 [*Kennett and Engdahl*, 1991] the signal at −45 s cannot be detected, but it is present in the synthetics for the model with a strong (0.3 km/s) S velocity reduction at a depth of 360 km. To reconcile this model with the known data on cratonic roots, velocities at depths less than 330 km are taken higher than in IASP91. The synthetic signal is focused at 0.8 s/deg, slightly different from 0.6 s/deg in the actual data. The discrepancy is thought to be negligible, and it can be further reduced by reducing velocities above the discontinuity. The time of the synthetic signal is close to that in the actual data. The synthetic signal is 1.5 times weaker than the actual one, but the actual signal is probably enhanced by a local site effect: the amplitude of the phase converted at the Moho is larger than the normal amplitude

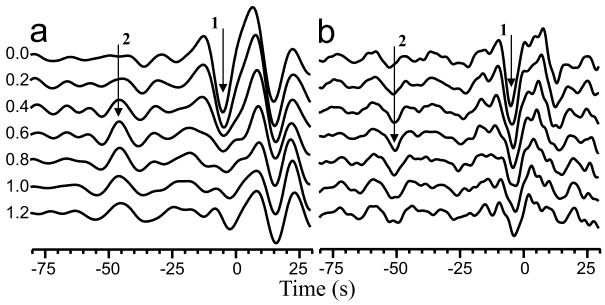


**Figure 2.** $P_c(t)$ for station BOSA in the back azimuths of 30°–60° (a) and 230°–260° (b). Reference epicentral distance is 80° and 82°, respectively. Each trace corresponds to the differential slowness (in *s*/°) attached on the left. Origin of time scale corresponds to the arrival of the S phase. The detected Sp phases are marked by arrows.

**Table 1.** Representative Recordings at BOSA

| Date | *Lat*° | *Lon*° | Dep | *Dis*° | *Baz*° |
|---|---|---|---|---|---|
| 18/09/93 | 36.48 | 71.80 | 118 | 78.0 | 36.7 |
| 01/05/94 | 37.10 | 66.85 | 24 | 76.1 | 33.4 |
| 08/08/94 | 24.76 | 94.97 | 146 | 85.7 | 59.0 |
| 25/10/94 | 36.25 | 71.00 | 258 | 77.6 | 36.3 |
| 08/10/95 | 41.23 | 71.87 | 20 | 81.7 | 33.9 |
| 03/02/96 | 27.15 | 100.28 | 15 | 90.9 | 59.3 |
| 19/11/96 | 35.45 | 77.86 | 15 | 80.8 | 41.3 |
| 20/03/97 | 30.79 | 67.79 | 15 | 71.3 | 38.4 |
| 10/05/97 | 33.58 | 60.02 | 15 | 70.2 | 30.1 |
| 25/06/97 | 34.04 | 59.53 | 15 | 70.1 | 29.8 |
| 14/03/98 | 29.95 | 57.60 | 15 | 66.1 | 30.5 |
| 28/03/99 | 30.38 | 79.21 | 15 | 78.2 | 45.6 |

Dep is depth in km, Dis is epicentral distance, Baz is back azimuth.

(0.17 versus 0.1). For the top of the low-velocity layer at a representative epicentral distance of 80°, the Sp ray piercing point is located 500 km to the North-East of the seismograph station (Figure 1).

[9] In the stack for IASP91 model there is no visible signal from '410 km' discontinuity. This can be explained as follows. In a distance interval around 80° the S wavetrain is composed of phases S, SKS and ScS with different slownesses. Coherence between the composite wavetrains at the surface and at a large depth can be low. Then the Sp phase can not be transformed by deconvolution into the standard 'bump' and contribute to the signal in the stack. Magnitudes and critical depths of this effect are different for different groups of seismic events. The data in Figure 3 indicate that this set of events is unfavourable for detection of the Sp phase from 410 km depth, and at a depth around 410 km our model is not constrained by the observations.

[10] Recordings of stations SUR and TSUM in southern Africa appeared to be more noisy and too few, but at station LBTB we detected mantle signals (Figure 5). In the azimuthal sector of 30°–60° in the stack of 18 recordings, almost all of them in a distance interval between 68° and 89° there are Sp phases from the Moho (at −5 s), '410-km' discontinuity (at −53 s) and from a depth of 280–300 km (at −36 s). The latter is with inverse polarity and corresponds to the top of a low-velocity layer. Its amplitude (0.037) is large in comparison with the standard error (0.012). In the azimuth of 230°–270° with 37 events in a distance interval from 79° to 104° the only detectable mantle signal is from '410-km' discontinuity. Again, indication of the low-velocity layer is found only to the North-East of the station.

[11] We investigated with the same technique the upper mantle beneath the Precambrian platform of north America (station HRV), East-European platform (KIEV and OBN) and the Siberian platform (NRIL). Evidence of the deep low-velocity layer has been

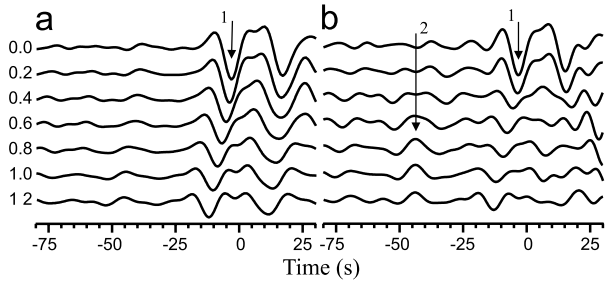


**Figure 3.** The same as in Figure 2a but for synthetic seismograms. The seismograms are calculated for standard model IASP91 (a) and model with a low S velocity layer (b). Mantle S velocities in both models are shown in Figure 4.

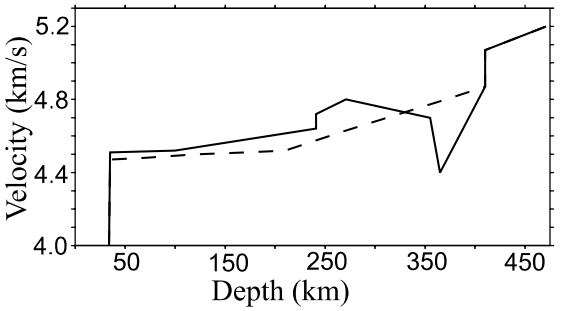


**Figure 4.** Mantle S velocities adopted for modeling. The resulting synthetics are shown in Figure 3.

found only in the recordings of station NRIL (coordinates 69.50 N, 88.44 E). In the stack of 49 recordings in the back-azimuth sector of 140°–180° with almost all events in the epicentral distance interval from 65° to 82° (Figure 6) there is clear evidence of the Sp phases from the Moho (at −5 s), '410-km' discontinuity (at −57 s), and a discontinuity at a depth around 350 km (at −49 s). Polarity of the latter is opposite to the others, which means that it is converted from the top of a low-velocity layer. Both mantle phases are focused at a right differential slowness (0.6 s/deg) and their amplitudes (around 0.03) are much larger than the standard error (0.01). Dominant periods in the signal at −49 s (around 15 s) are longer than at −57 s (around 10 s).

## 4. Discussion and Conclusions

[12] We presented evidence of a super-deep low velocity layer in the upper mantle of southern Africa (stations BOSA and LBTB) and Tunguska basin of the Siberian platform (station NRIL). In southern Africa the layer is found north-east of stations BOSA and LBTB. No indications of it is found west and south-west of the stations. In the best data (those of station BOSA) the layer is found at the same depth as previously from the analysis of the Ps phases [*Vinnik et al.*, 1996]. Both studies are in remarkable agreement, although the discontinuity in Figure 4 is much stronger than found previously. The difference in strength can be attributed to a difference in locations: the region sampled with the Sp phases is shifted to the East. A smooth upper boundary of the low-velocity layer can be another reason: wavelengths of the Sp phases are longer and less sensitive to the sharpness of the discontinuity.

[13] With the aid of the Sp phases indications of the low-velocity layer have been found in two regions, but they could not be found in a few other regions. Applications of the S receiver function technique still are few, but there are many observations of the mantle Ps phases with the P receiver function technique. Beyond southern Africa, indications of the super-deep low-velocity

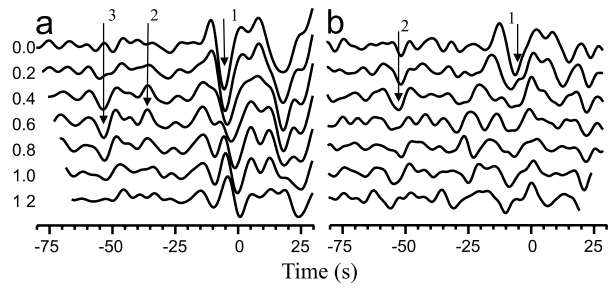


**Figure 5.** The same as in Figure 2, but for station LBTB in the back azimuths of 30°–60° (a) and 230°–270° (b). Reference epicentral distance is 80°.

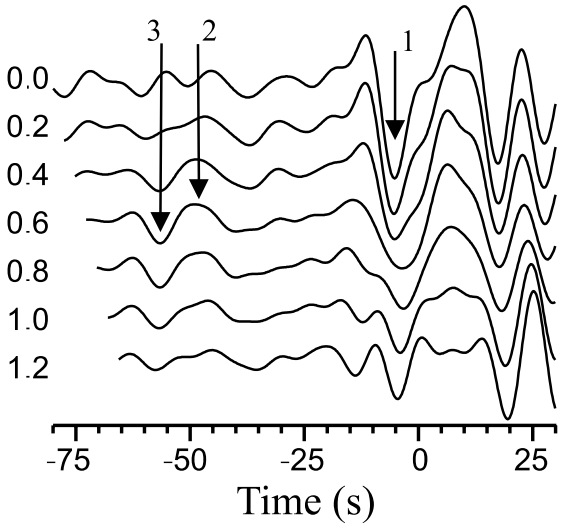


**Figure 6.** The same as in Figure 2 but for station NRIL in the back azimuths of 140°–180°. Reference epicentral distance is 75°.

layer have been reported only for station ATD (coordinates 11.53 N, 42.85 E) in Afar region [*Chevrot et al.*, 1999]. No evidence of this layer has been found in the Ps phases at station NRIL. There can be two reasons for this. The low-velocity layer is found a few hundred kilometres to the SSE of station NRIL, but it can disappear in the region sampled by the Ps phases in a close neighbourhood of the station. Periods of the Ps phases are relatively short, and the signal from a smooth upper boundary of the low-velocity layer can be too weak for a detection.

[14] In any case the indications of the super-deep low-velocity layer are rare in both Ps and Sp phases. Three regions with evidence of this layer are remarkable by large-scale eruptions of continental flood basalts. In southern Africa the Karoo flood basalt province is located east of the dash line in Figure 1. The original lavas are eroded, but they probably covered 2 million km$^2$ [*Cox*, 1972]. Ages of the eruptions are around 180 Ma and 190 Ma. Seismic velocities in the upper mantle of the eastern Kaapvaal craton are relatively low [*James et al.*, 2001]. The anomaly was attributed to the Bushveld magmatic event of 2.05 Ga age. However, the Karoo magmatic event is much younger, and its influence on the presently observed properties of the upper mantle should be stronger than the effect of the Bushveld event. Siberian traps in the Tunguska Basin where the low-velocity layer is found from the data of station NRIL are around 250 Ma old, and their area is more than 2.5 million km$^2$ [*Zolutkhin and Al'mukhamedov*, 1988]. Evidence of the low-velocity layer in the data of station ATD is related to the province of extensive flood basalts in Ethiopia and on the Arabian plate. The main episode of flood basalt volcanism was during the period from 30 to 20 Ma [*White and McKenzie*, 1989].

[15] Origin of the flood basalts is attributed to decompression melting of anomalously hot mantle brought by plumes [*White and McKenzie*, 1995]. Temperature in the mantle at the time of the eruptions was enhanced by about 150°C [*White and McKenzie*, 1995]. If the low-velocity is of thermal origin, the temperature in the layer, as found from the appropriate temperature derivatives [*Karato*, 1993], is enhanced by roughly the same value. This value is too high for the anomaly about 200 Ma old. Alternatively, the low velocity could be caused by anomalous composition. This layer can be enriched in sodium, potassium, iron, incompatible elements and volatiles [*Gasparik*, 1992]. Rocks in this depth range may contain water stored in hydrous silicates [*Thompson*, 1992]. Hydrous phases may have lower velocities compared to their

anhydrous equivalents [*Tuburczy et al.*, 1991]. Moreover, if temperature in the mantle is enhanced by a thermal plume, water can be released by dehydration. Then temperature of the mantle solidus is lowered, and melts can be formed.

[16] Whatever the origin of the low velocity, a correlation between the locations of the low-velocity layer and of the continental flood basalts up to 250 Ma old suggests that the layer migrates with the plates. While this is very surprising with respect to conventional wisdom, a similar conclusion (coupled motion of the lithosphere and of the underlying upper mantle) was derived from a tomographic model of the upper mantle beneath the Parana flood basalts 137–127 Ma old in South America [*VanDecar et al.*, 1995]. Apparently the coupled motion is characteristic of the continents on both sides of the Atlantic.

[17] **Acknowledgments.** L. Vinnik is partially supported by the RFBR grant 01-05-64243. Comments from an anonymous reviewer and Hanneke Paulssen are appreciated.

## References

Chevrot, S., L. Vinnik, and J.-P. Montagner, Global scale analysis of the mantle Pds phases, *J. Geophys. Res.*, *104*, 20,203–20,219, 1999.

Cox, K. G., The Karoo volcanic cycle, *J. Geol. Soc. London*, *128*, 311–336, 1972.

Farra, V., and L. Vinnik, Upper mantle stratification by P and S receiver functions, *Geophys. J. Int.*, *141*, 699–712, 2000.

Freibourger, M., J. B. Gaherty, and T. H. Jordan, Structure of the Kaapvaal craton from surface waves, *Geophys. Res. Lett.*, *28*, 2489–2492, 2001.

Fuchs, K., and G. Mueller, Computation of synthetic seismograms with the reflectivity method and comparison with observations, *Geophys. J.R.A.S.*, *23*, 417–433, 1971.

Gasparik, T., Enstatite-jadeite join and its role in the Earth's mantle, *Contrib. Mineral. Petrol.*, *111*, 283–298, 1992.

James, D. E., M. J. Fouch, J. C. VanDecar, and N. van der Lee, Tectospheric structure beneath southern Africa, *Geophys. Res. Lett.*, *28*, 2485–2488, 2001.

Karato, S., Importance of anelasticity in the interpretation of seismic tomography, *Geophys. Res. Lett.*, *20*, 1623–1626, 1993.

Kennett, B. L. N., and E. R. Engdahl, Traveltimes for global earthquake location and phase identification, *Geophys. J. Int.*, *105*, 429–465, 1991.

Thompson, A. B., Water in the mantle, *Nature*, *358*, 295–302, 1992.

Tuburczy, J. A., T. S. Duffy, T. J. Ahrens, and M. A. Lange, Shock wave equation of state of serpentine to 150 GPa: Implications for the occurence of water in the earth's lower mantle, *J. Geophys. Res.*, *96*, 18,011–18,027, 1991.

VanDecar, J. C., D. E. James, and M. Assumpcao, Seismic evidence for a fossil mantle plume beneath South America and implications for plate driving forces, *Nature*, *378*, 25–31, 1995.

Vinnik, L. P., R. W. E. Green, L. O. Nicolaysen, G. L. Kosarev, and N. V. Petersen, Deep structure of the Kaapvaal craton, *Tectonophysics*, *262*, 67–75, 1996.

White, R., and D. McKenzie, Magmatism of rift zones: the generation of volcanic continental margins and flood basalts, *J. Geophys. Res.*, *94*, 7685–7729, 1989.

White, R., and D. McKenzie, Mantle plumes and flood basalts, *J. Geophys. Res.*, *100*, 17,543–17,585, 1995.

Zolutkhin, V. V., and A. I. Al'mukhamedov, Traps of the Siberian platform, in *Continental flood basalts*, edited by D. J. Macdughall, pp. 273–310, Kluwer Acad. Nouvell, Mass., 1988.

V. Farra, Department de Sismologie, CNRS UMR 7580, Institut de Physique du Globe, 4 Place Jussieu, Paris 75252 cedex, France. (farra@ipgp.jussieu.fr)

L. Vinnik, Institute of Physics of the Earth, B. Grouzinskaya 10, Moscow 123995, Russia.